CNWRA 95-004

# PROGRESS TOWARD A FRACTAL REPRESENTATION OF ROCK JOINT ROUGHNESS

*Prepared for*

**Nuclear Regulatory Commission**
**Contract NRC-02-93-005**

*Prepared by*

**Center for Nuclear Waste Regulatory Analyses**
**San Antonio, Texas**

**January 1995**

CNWRA 95-004

# PROGRESS TOWARD A FRACTAL REPRESENTATION OF ROCK JOINT ROUGHNESS

*Prepared for*

**Nuclear Regulatory Commission**
**Contract NRC-02-93-005**

*Prepared by*

**S.M. Hsiung**
**A. Ghosh**
**A.H. Chowdhury**

**Center for Nuclear Waste Regulatory Analyses**
**San Antonio, Texas**

**January 1995**

# ABSTRACT

Currently available rock joint models were developed based on data taken under unidirectional pseudostatic loading conditions. These models cannot be used to adequately predict the joint response during reverse shearing. The primary reason for this is that the joint roughness representations used in these models do not appear to contain the joint characteristics that are responsible for the joint reverse shearing behavior observed in the laboratory. A proper representation for rock joint roughness appears to be needed.

Self-affine fractal properties of Barton's ten standard profiles for the joint roughness coefficient (JRC) were analyzed with the ultimate goal of relating the JRC values with the fractal properties of rock profiles. Four different methods were adopted in the study for calculation of fractal properties. The applicability of these methods was tested using the fractional Brownian motion functions with Hurst exponent, H, varying from 0.5 to 0.9. Contrary to the common belief that a larger fractal dimension, D, should correspond to a higher JRC value, all four methods consistently predict a decreasing trend of JRC values with increase in fractal dimension. This finding suggests that using fractal dimension alone for rock profile characterization is not sufficient. The intercept of the fractal model was found to be representative of the local trend (long wavelengths) of a rock profile that controls the shear behavior of rock joints at laboratory scales. To uniquely define a joint profile, both the fractal dimension and the intercept are needed. Even considering these two parameters in evaluating the ten profiles, this study has shown that not all of the ten standard profiles are representative of the roughness classes as suggested. Consequently, it has not been possible to develop a valid systematic relationship between the fractal properties and JRC values of the ten profiles. Barton's ten profiles will need to be revised to meet more rigorous requirements or an alternate approach is needed for relating the roughness of a joint surface and its fractal properties.

# CONTENTS


Section Page

FIGURES . . . . . vii
ACKNOWLEDGMENTS . . . . . ix
EXECUTIVE SUMMARY . . . . . xi

1 INTRODUCTION . . . . . 1-1
1.1 BACKGROUND . . . . . 1-1
1.2 OBJECTIVE AND SCOPE . . . . . 1-1

2 ROCK JOINT RESPONSE UNDER PSEUDOSTATIC AND DYNAMIC LOADS . . . . . 2-1
2.1 CYCLIC PSEUDOSTATIC LOAD . . . . . 2-1
2.2 DYNAMIC LOAD . . . . . 2-1

3 DEVELOPMENT OF CHARACTERIZATION TECHNIQUE FOR ROCK JOINT ROUGHNESS . . . . . 3-1
3.1 DIVIDER METHOD . . . . . 3-1
3.2 VARIOGRAM METHOD . . . . . 3-2
3.3 SPECTRAL METHOD . . . . . 3-3
3.4 ROUGHNESS-LENGTH (RMS) METHOD . . . . . 3-3
3.5 METHOD VERIFICATION . . . . . 3-3
3.6 EVALUATION OF BARTON'S TEN PROFILES . . . . . 3-4

4 NEED FOR ALTERNATIVE APPROACH . . . . . 4-1

5 SUMMARY . . . . . 5-1

6 REFERENCES . . . . . 6-1

# FIGURES


| Figure | | Page |
|---|---|---|
| 2-1 | Shear stress response of test no. 17 specimen under pseudostatic cyclic loading condition as a function of normal stress | 2-2 |
| 2-2 | Joint dilation curves for test no. 17 specimen under pseudostatic cyclic loading condition as a function of normal stress | 2-2 |
| 2-3 | Shear stress versus shear displacement curve of a joint under a harmonic load with 1.4-Hz input frequency and 12.7-mm input displacement amplitude (load cycle numbers are indicated in the figure) | 2-3 |
| 2-4 | Shear stress versus shear displacement curve of a joint under an earthquake load with a maximum input displacement amplitude of 25.4 mm (load cycle numbers are indicated in the figure) | 2-3 |
| 2-5 | Input earthquake displacement time history | 2-4 |
| 2-6 | Shear stress versus shear displacement response as a function of applied normal load for various joint specimens | 2-6 |
| 2-7 | Joint normal displacement (dilation) versus shear displacement of a joint under a harmonic load with 1.4-Hz input frequency and 12.7-mm input displacement amplitude | 2-7 |
| 2-8 | Joint normal displacement (dilation) versus shear displacement of a joint under an earthquake load with maximum input displacement amplitude of 25.4 mm | 2-7 |
| 2-9 | Effect of input frequency (shearing velocity) on peak joint shear strength | 2-8 |
| 2-10 | Effect of input frequency (shearing velocity) on joint shear strength during reverse shearing | 2-9 |
| 3-1 | Comparison of Hurst exponents calculated using the four methods with the expected values | 3-4 |
| 3-2 | Roughness profiles and the corresponding range of JRC values | 3-5 |
| 3-3 | Relation of JRC and the corresponding fractal dimension calculated from four different methods | 3-6 |
| 3-4 | Plot of fractal models for Barton's ten profiles from the variogram method | 3-7 |
| 3-5 | Plot of fractal models for Barton's ten profiles from the spectral method | 3-8 |
| 3-6 | Plot of fractal models for Barton's ten profiles from the RMS method | 3-8 |

# ACKNOWLEDGMENTS

The authors thank Dr. W.C. Patrick and P. Mackin for their review of this report. This report was prepared to document work performed by the Center for Nuclear Waste Regulatory Analyses (CNWRA) for the Nuclear Regulatory Commission (NRC) under Contract No. NRC-02-93-005. The activities reported here were performed on behalf of the NRC Division of Waste Management. This report is an independent product of the CNWRA and does not necessarily reflect the views or regulatory position of the NRC.

All CNWRA-generated original data contained in this paper meet the quality assurance requirements described in the CNWRA Quality Assurance Manual. Sources for other data should be consulted for determining the level of quality for those data.

# EXECUTIVE SUMMARY

The results of an extensive laboratory study of the cyclic pseudostatic and dynamic behavior of rock joints, which was conducted as a part of the ongoing Rock Mechanics Research Project at the Center for Nuclear Waste Regulatory Analyses (CNWRA), have indicated a distinct difference between joint shear behavior during forward shearing and reverse shearing, whether a rock joint is subjected to a cyclic pseudostatic or dynamic shear loading. This finding has severely limited the utility of the commonly used rock joint models for adequately describing joint behavior under cyclic pseudostatic or dynamic loading conditions. These rock joint models were extended to predict the joint reverse shearing behavior by assuming that the reverse shearing would follow the same rule as the forward shearing. This assumption is found to be inconsistent with the experimental findings.

A major effort has been undertaken by the CNWRA on behalf of the Nuclear Regulatory Commission (NRC) Division of Waste Management in developing a rock joint model that can be used for adequate representation of rock joint cyclic behavior. This rock joint model will include mathematical representations of joint shear and dilation behavior. This report documents the progress to-date on developing a methodology for characterizing rock joint surface profiles and establishing a relationship between the characterized joint profile and the joint roughness concept. Such relationship will form the basis for the development of a rock joint model.

The approach adopted uses the theory of fractal geometry to characterize the ten standard profiles proposed by Barton (1973). The objective was to make use of the concept of joint roughness coefficient (JRC), developed by Barton (1973) and accepted by the International Society for Rock Mechanics (ISRM) (1978) as the standard for representing surface roughnesses, where the relationship has been established between JRC and rock joint model parameters such as friction angle and rock joint degradation. Since a rational rock joint model needs to adequately account for the roughness of the joint surface the plan was to determine the fractal properties of the ten standard profiles using the self-affine fractal method and then to establish the relationship between the fractal properties and the rock joint model parameters. Four methods [i.e., divider, variogram, spectral, and roughness-length (RMS)] were used for the determination of fractal properties, initially the fractal dimension, D. Contrary to the common belief that a larger D should correspond to a higher JRC value, the results from all four methods show a consistent trend of a profile with a higher JRC value having a smaller D value. Thus, the D value alone cannot be used to uniquely characterize the roughness of a rock joint. The intercept of the fractal model was found to be representative of the local trend (long wavelengths) of a rock profile that controls the overall shear and dilation behavior of rock joints. To uniquely define a joint profile, both the fractal dimension and the intercept are needed. Even considering these two parameters, this study has shown that not all of the ten standard profiles are representative of the roughness classes as proposed by Barton (1973). It is, therefore, not possible to establish a valid systematic relationship between the fractal properties and the JRC values of the ten profiles.

An alternate approach is considered to be necessary for relating the roughness of a joint surface and its fractal properties; the fractal dimension and the intercept. Two alternatives are currently under study. One is to modify the standard profiles, with JRC values between 6 and 16, as appropriate. The other approach is to develop a new basis for correlating the fractal dimension and intercept of a rock joint with its joint model parameters such as friction angle and rock joint degradation under shear.

# 1 INTRODUCTION

## 1.1 BACKGROUND

In 1987, the U.S. Congress designated Yucca Mountain, in southern Nevada, as the only site to be characterized to determine its suitability for constructing a repository for high-level nuclear waste (HLW). The proposed repository horizon is about 300 m beneath Yucca Mountain, in a densely welded prominently vertically and subvertically jointed tuff. The unit was chosen as the proposed repository horizon because of its thickness, lateral continuity, dense welding, and its location in the unsaturated zone about 200 to 400 m above the water table.

Analyses of the behavior of underground structures in hard rocks, such as those proposed at Yucca Mountain, which contain discontinuities such as faults, joints, shear zones, and beddings, show that the shear behavior of these discontinuities is a primary determinant of rock mass deformation and the stability of the underground structures under various loading conditions. One important loading condition that could potentially affect the preclosure and postclosure performance of a repository is repeated ground motion due to seismic activities (Kana et al., 1991; Nuclear Waste Technical Review Board, 1992). The fundamental failure mechanism for an excavation in a jointed rock mass subjected to repetitive seismic loading is the accumulation of shear displacements at the major pervasive features such as joints and faults (Hsiung et al., 1992a;b). Conditions for slip on joints or for the sliding of individual blocks from the boundaries of excavations are governed by the shear strengths that can be developed by the discontinuities. Specific seismic implications for repository design and performance may include cumulative effects of repetitive seismic loads on: (i) emplacement drift stability; (ii) underground opening stability; and (iii) creation of preferential water pathways to connect the emplacement area with perched water zones, neighboring steep hydraulic gradient zones, or the condensation area above the emplacement area.

The results of an extensive laboratory study of the cyclic pseudostatic and dynamic behavior of rock joints, which was conducted as a part of the ongoing Rock Mechanics research project at the Center for Nuclear Waste Regulatory Analyses (CNWRA), have indicated a distinct difference between joint shear behavior during forward shearing and reverse shearing, whether a rock joint is subjected to a cyclic pseudostatic or dynamic shear loading. (A concise definition for forward shearing and reverse shearing is provided in a later section). This observation has severely limited the utility of commonly used rock joint models, which were developed based primarily on experimental data taken under unidirectional pseudostatic loading conditions, in predicting joint performance under cyclic pseudostatic and dynamic loading conditions (Hsiung et al., 1994b). These rock joint models were extended to predict the joint reverse shearing behavior by assuming that reverse shearing would follow the same rule as forward shearing. This assumption is not consistent with the experimental results (Hsiung et al., 1994a; Wibowo et al., 1992; Huang et al., 1993; Jing et al., 1992). These experimental results have suggested that the representations of the joint roughness used in the existing rock joint models do not adequately reflect the actual joint characteristics that control the reverse shearing behavior. A new or modified joint roughness representation is needed to allow a rock joint model to adequately predict the reverse shearing behavior.

## 1.2 OBJECTIVE AND SCOPE

The objective of this study is to develop a rock joint model using the experimental results of the Rock Mechanics research project (Hsiung et al., 1994a) that can be used for representation of rock

joint cyclic behavior. The activities associated with the development of a rock joint model for predicting the cyclic pseudostatic and dynamic behavior of a jointed rock mass include:

(i) Developing a methodology for characterizing rock joint surface profiles and establishing a relationship between the characterized joint profile and the joint roughness concept

(ii) Developing a model for joint roughness degradation due to joint shearing

(iii) Developing a mathematical representation of joint shear behavior utilizing the relationship developed in item (i) and the degradation model developed in item (ii)

(iv) Developing a mathematical representation of joint dilation behavior utilizing the relationship developed in item (i) and the degradation model developed in item (ii), and

(v) Testing the validity of the rock joint model developed

This progress report is intended to document the activity and results to date for item (i). Chapter 2 gives a brief discussion regarding the experimental results obtained at the CNWRA while studying the joint cyclic shear behavior and the need for a method for characterizing rock joint surfaces that will capture the characteristics governing the joint shear behavior during reverse shearing. Chapter 3 discusses the development of such a method using the self-affine fractal approach along with the problems encountered in correlating JRC with the fractal properties of the ten standard profiles proposed by Barton (1973). Chapter 4 outlines current thinking on further rock joint model development in the light of the results obtained in Chapter 3.

# 2 ROCK JOINT RESPONSE UNDER PSEUDOSTATIC AND DYNAMIC LOADS

The rock joint specimens used for the cyclic pseudostatic and dynamic direct shear tests in the CNWRA experimental program (Hsiung et al., 1994a) were collected from the Apache Leap site near Superior, Arizona. The rock at the Apache Leap site is a vitrified and densely welded tuff that is moderately to heavily jointed. A large-diameter core drilling technique was used for sample collection. From these cores, rock joint specimens were prepared to a predetermined size such that the rock block on one side of the joint had dimensions of $305 \times 203 \times 102$ mm and the rock block on the other side of the joint had dimensions of $203 \times 203 \times 102$ mm. The joint surfaces on both rock blocks were matched when the rock block with smaller size (top block) was seated at the center of the larger size rock block (bottom block).

## 2.1 CYCLIC PSEUDOSTATIC LOAD

During a cyclic pseudostatic direct shear test, the top block was sheared a distance of about 2 in. (50.8 mm) in one direction followed by a reversal of shearing back to the original starting position under a predetermined constant normal stress and at a constant velocity of about $4.2 \times 10^{-2}$ mm/sec. The same process could be repeated on the same joint specimen under a different normal stress level. To aid the discussion, the term "forward shearing" is used throughout this report to indicate that the top rock block moves away from its original position while the term "reverse shearing" denotes the top rock block moves toward its original position, regardless of the absolute direction of movement.

Figure 2-1 shows the shear stress response for test no. 17 (Hsiung et al., 1994a) under various normal stress levels. The test sequence followed an ascending order with respect to the normal stress. The curve with the 1-MPa normal stress (the first cycle of shearing) illustrates the shear behavior of an originally undamaged (fresh) joint and shows a distinct peak shear strength at the early stage of the shear cycle. The shear strength of the joint gradually reduces to a residual value at greater shear displacements. No distinct peak shear strength was observed for other cycles of shearing. Figure 2-1 also indicates a gradual increase in shear strength during reverse shearing when the top block was approaching its original position. Another feature that can be observed in this figure is that the shear strength during the reverse shearing is smaller than the shear strength during the forward shearing.

The relation between normal displacement (dilation) and shear displacement for test no. 17 is given in Figure 2-2. This figure indicates that joint dilations at various normal stresses increase during forward shearing. For reverse shearing, there is some degree of hysteresis with the joint dilation decreasing towards zero from below the dilation curve of forward shearing. In general, for repeated shear cycles, the amount of joint dilation decreased with increasing normal stress.

## 2.2 DYNAMIC LOAD

Figures 2-3 and 2-4 show the characteristic plot of joint shear stress versus joint shear displacement under harmonic and earthquake loading conditions, respectively. The harmonic load for Figure 2-3 was generated from a prescribed shear displacement drive input in a sinusoidal wave form. The frequency and amplitude of the harmonic input motion were 1.4 Hz and 12.7 mm, respectively. The earthquake input motion used in Figure 2-4 is shown in Figure 2-5 with a nominal maximum displacement amplitude of 25.4 mm and a dominant frequency of about 0.5 Hz. This displacement input

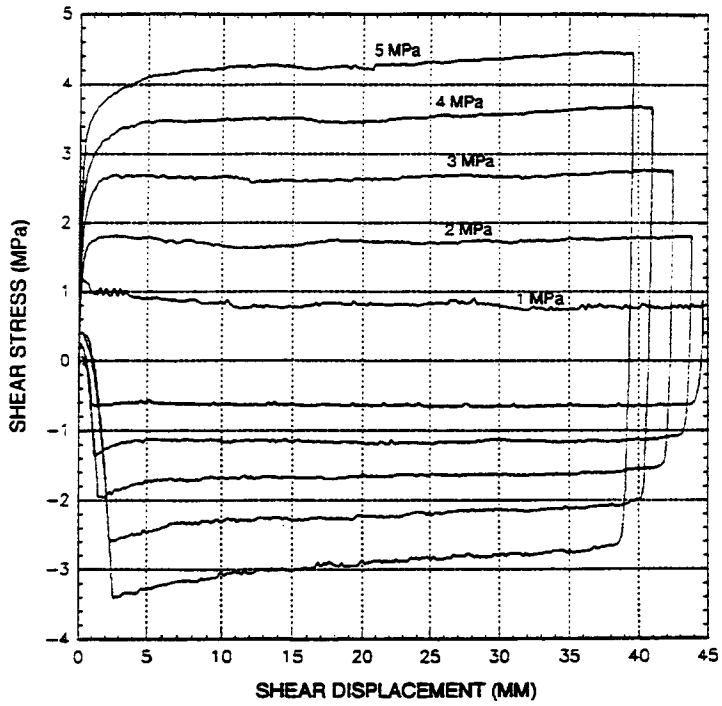


**Figure 2-1. Shear stress response of test no. 17 specimen under pseudostatic cyclic loading condition as a function of normal stress**

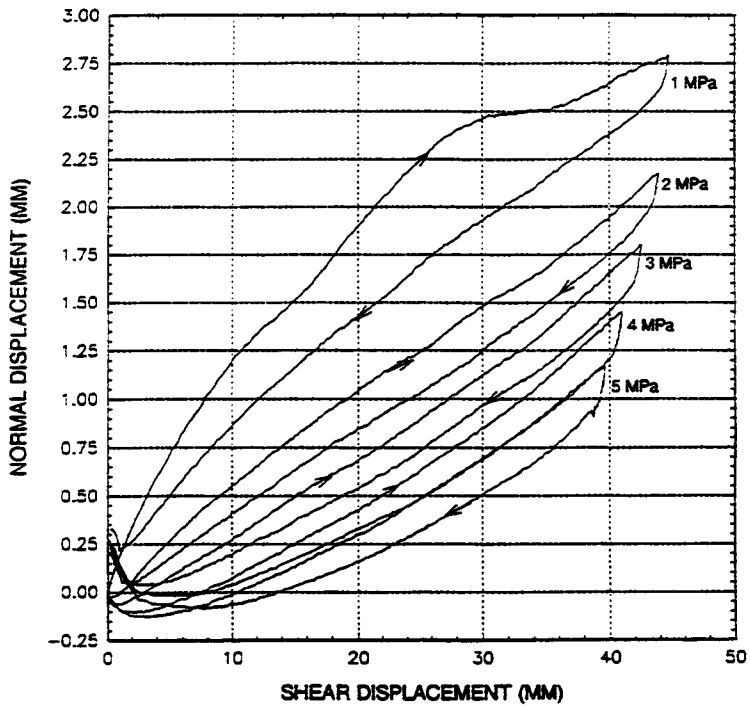


**Figure 2-2. Joint dilation curves for test no. 17 specimen under pseudostatic cyclic loading condition as a function of normal stress**

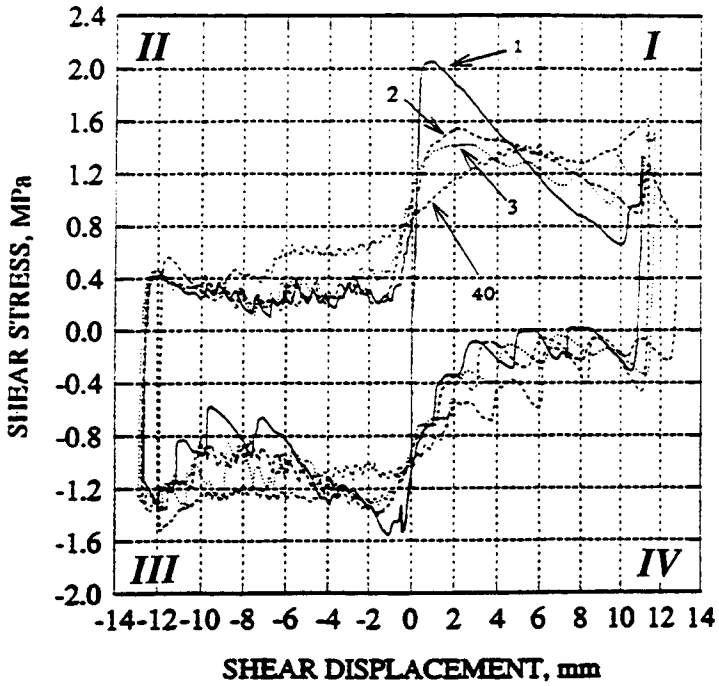


**Figure 2-3. Shear stress versus shear displacement curve of a joint under a harmonic load with 1.4-Hz input frequency and 12.7-mm input displacement amplitude (load cycle numbers are indicated in the figure)**

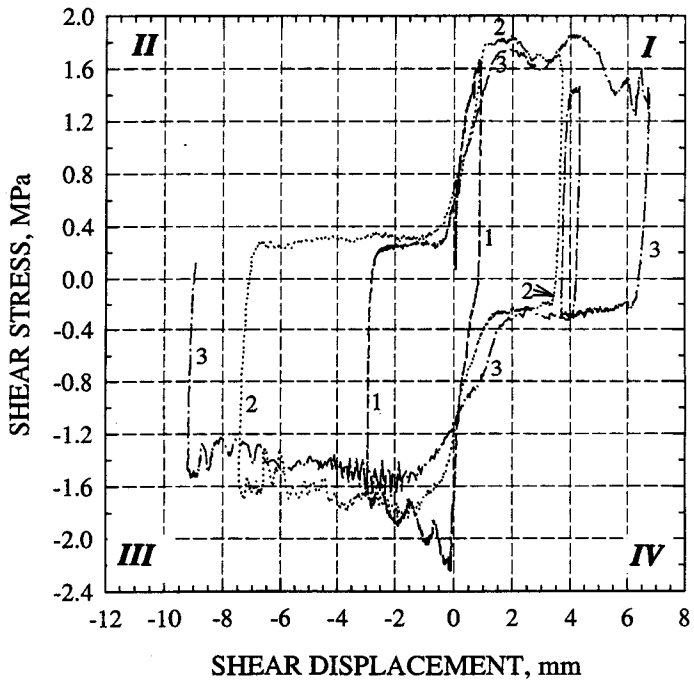


**Figure 2-4. Shear stress versus shear displacement curve of a joint under an earthquake load with a maximum input displacement amplitude of 25.4 mm (load cycle numbers are indicated in the figure)**

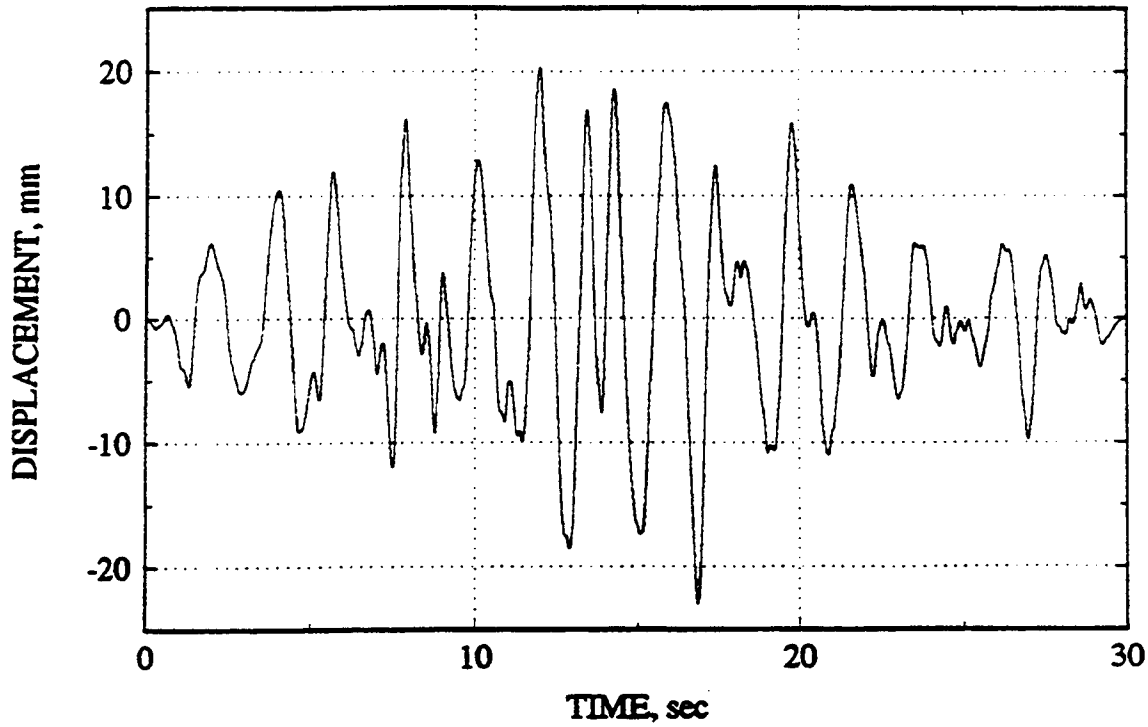


**Figure 2-5. Input earthquake displacement time history**

signal was developed based on the acceleration response signal recorded from the Guerrero accelerograph array for the earthquake of September 19, 1985, in Mexico. The development of this displacement input has been discussed by Hsiung et al. (1994a). All figures include the test results of the first three cycles and Figure 2-3 also includes the result of the 40th cycle.

For Figures 2-3 and 2-4, the experiment started with shearing the top rock block from its original position (represented as the zero shear displacement in the figures) toward one end of the bottom rock block until a predetermined maximum value of shear displacement (based on the input displacement time history) was reached. The corresponding shear stress versus shear displacement characteristic curve with this portion of shearing is shown in the first quadrant of the figures (i.e., clockwise progression around the figure). After the maximum shear displacement in the first quadrant was reached, the top rock block began to move backward and eventually past its original position. The corresponding shear stress versus shear displacement characteristic curves are presented in the fourth and third quadrants of the figures, respectively. After the maximum shear displacement in the third quadrant was reached, the top rock block moved again back to its original position to complete a cycle of shear motion, and the associated shear stress versus shear displacement characteristic curve is presented in the second quadrant of the figures. This process was repeated for a number of cycles. As shown in the figures, the shear stress is denoted as positive when shearing is in one direction and negative when shearing is in the opposite direction. Consequently, the sign for the shear stress denotes the direction of the shear instead of the magnitude of the shear stress.

A peak joint shear strength was observed for the first cycle of both harmonic and earthquake tests if the jointed specimens used for the tests were never shear tested before or did not show signs of past shearing before specimen collection. This observation is consistent with the joint pseudostatic

behavior. The phenomenon of wear of the joint is also clearly shown in the figures as the shear stress (joint shear strength) decreases with the number of cycles.

As observed for the cyclic pseudostatic tests (Figure 2-1), one distinct feature of the shear stress versus shear displacement characteristic curve in Figures 2-3 and 2-4 is the nature of the smaller shear strength upon reverse shearing as compared to that of forward shearing (the first quadrant versus the fourth quadrant, the third quadrant versus the second quadrant). The equivalent input frequency for the cyclic pseudostatic test as shown in Figure 2-1 is about $2.1 \times 10^{-4}$ Hz. The same behavior was also reported by other researchers (Jing et al., 1992; Wibowo et al., 1992; Huang et al., 1993) for rock joint replicas under cyclic pseudostatic loads.

It also can be observed in Figures 2-3 and 2-4 that the shear stress curves are fluctuating instead of smooth during the course of forward and reverse shearing. These variations can be better characterized as stick-slip (chatter) behavior. This chatter behavior may be related to the waviness of the joint surface and rock fragments broken from the joint surface (asperities), state of normal stress, frequency of the loading cycles (velocity of shear displacement), and the variation of strength of the asperities or rock fragments. During a shear test, when the shear stress is equal to the joint shear strength, joint slip begins. This joint slip will continue until asperities are encountered that tend to resist joint slip, that is, increase the joint shear resistance (strength). In such a situation, the joint stops slipping. The termination of a joint slip is the "stick" component of the phenomenon. The joint slip will not resume until the applied shear stress is increased to a level that overcomes this additional amount of joint shear resistance.

If the rock fragments between the joint surfaces are strong, additional shear stress is needed in order for the top rock block to crush or ride over them. As shown in Figure 2-6, which denotes the relation between the shear stress and shear displacement of different joints under pseudostatic cyclic loading condition, the joint chatter behavior was not as pronounced at a relatively lower normal stress level; in this figure, it is 1.0 MPa. However, when the input frequency was increased from $2.1 \times 10^{-4}$ Hz for the pseudostatic cyclic tests to 0.5 Hz for the earthquake tests, or more than 1.0 Hz for the harmonic tests, the chatter behavior becomes increasingly pronounced, although the applied normal stress was 1.0 MPa (Figures 2-3 and 2-4). It is also interesting to note that, in some cases of the dynamic tests, the chatter behavior continues even after a number of cycles of shearing. Small shear displacement may take place in the process of crushing or riding over the rock fragments since these rock fragments may not remain fixed in a place. Therefore, the stick component of the chatter behavior in this sense should be treated in a broader sense.

Figures 2-7 and 2-8 show the joint normal displacement versus shear displacement characteristic curves corresponding to Figures 2-3 and 2-4, respectively. The wear of the joint surfaces is a continuing process, as is evident in these figures, where the maximum joint normal displacement continues to decrease through the cycles of shearing. It is interesting to note that joint dilation (positive normal displacement) tends to decrease constantly during reverse shearing and may retain a small amount of dilation as the top rock block returns to its original position. The dilation curve is highly nonlinear but generally smooth for at least the first three cycles of the earthquake test results in Figure 2-8, as was the case for the pseudostatic test (Figure 2-2). However, for the harmonic test (Figure 2-7), many small-scale stick-slip oscillations were observed for many cycles. This observation gives an indication of the potential impact on joint dilation of input frequency, which may be related to the existence of small-size rock fragments created in the process of shearing. Under pseudostatic conditions or smaller input frequency conditions, shear stress tends to crush these rock fragments instead of riding over them. However, under conditions of high input frequencies or high shear velocity, the rock fragments are stronger and tend to

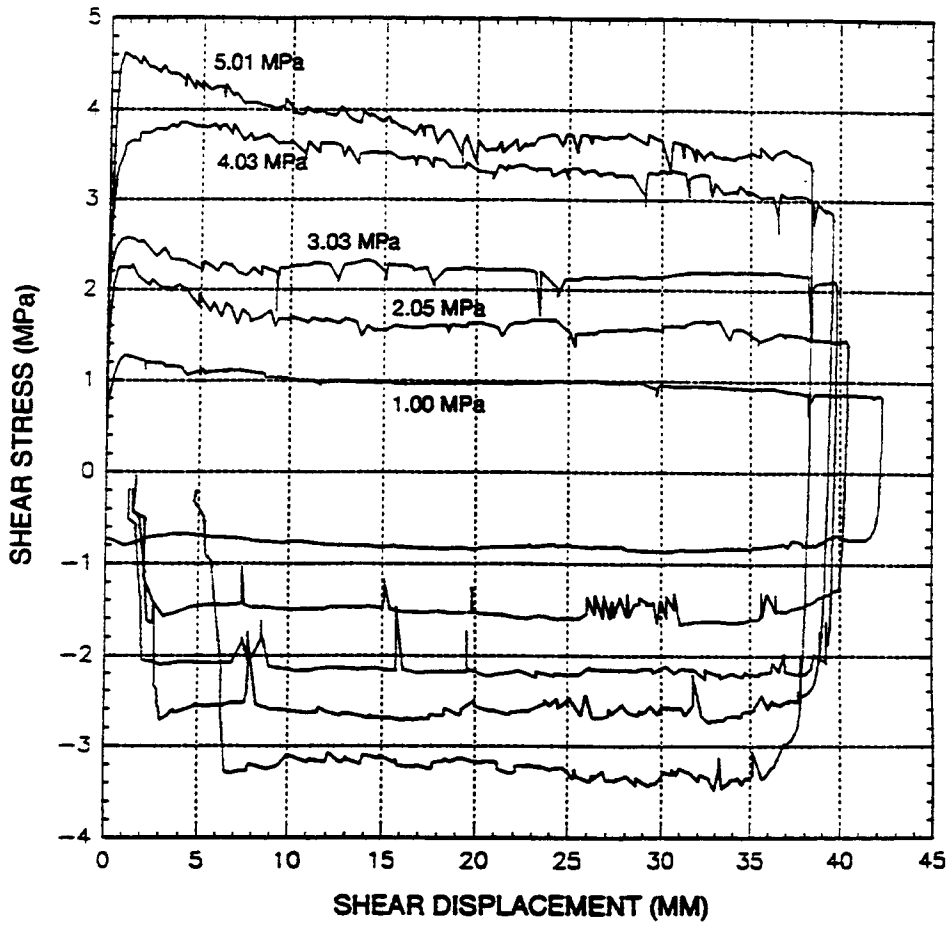


**Figure 2-6. Shear stress versus shear displacement response as a function of applied normal load for various joint specimens**

resist crushing and thus result in a temporary increase in normal displacement (the top block riding over these fragments). It is commonly understood that rock strength depends on loading rate and generally increases with increased loading rate. Once the fragments are crushed, the normal displacement tends to return to the original path. Judging from the overall joint shear behavior, the effect of the chatter component of joint performance is considered to be limited.

Because natural rock joints were used in direct shear tests under cyclic pseudostatic, harmonic, and earthquake loading conditions, a different joint specimen was needed for each test. As a result, the joint characteristics for each test were different. Therefore, it is impossible to evaluate directly the shearing velocity effect on the joint shear strength, unless some means is developed to account for the effect of different roughness. Figure 2-9 illustrates an approximate means for such an evaluation. Admittedly, the conclusion that can be drawn from this figure is at best an approximation, due to a number of uncertainties involved. However, it does give an indication of the potential shearing velocity effect on the peak shear strength. The horizontal axis of the figure represents the joint roughness coefficient (JRC) value calculated from the tilt test, while the vertical axis represents the JRC value calculated from the direct shear test results. Although it has been determined that the tilt test method

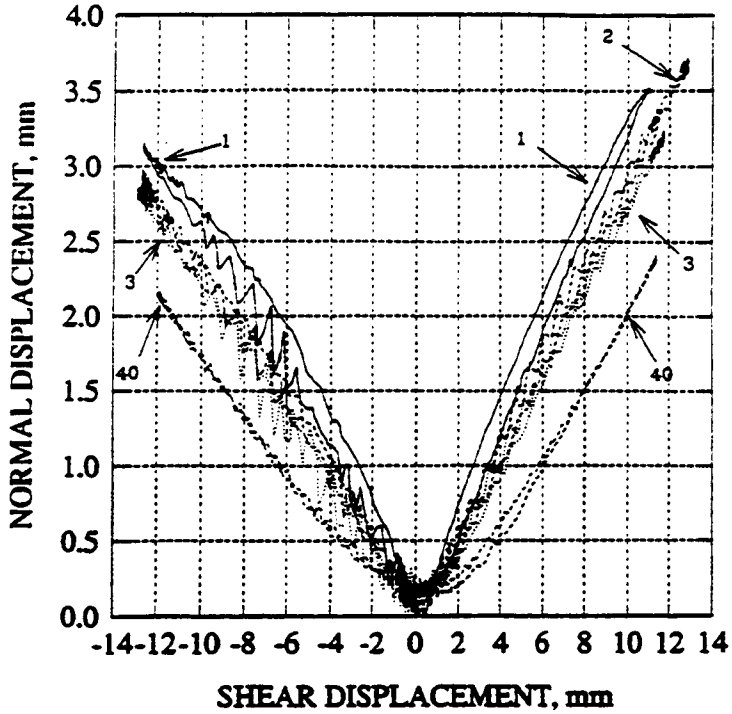


**Figure 2-7. Joint normal displacement (dilation) versus shear displacement of a joint under a harmonic load with 1.4-Hz input frequency and 12.7-mm input displacement amplitude**

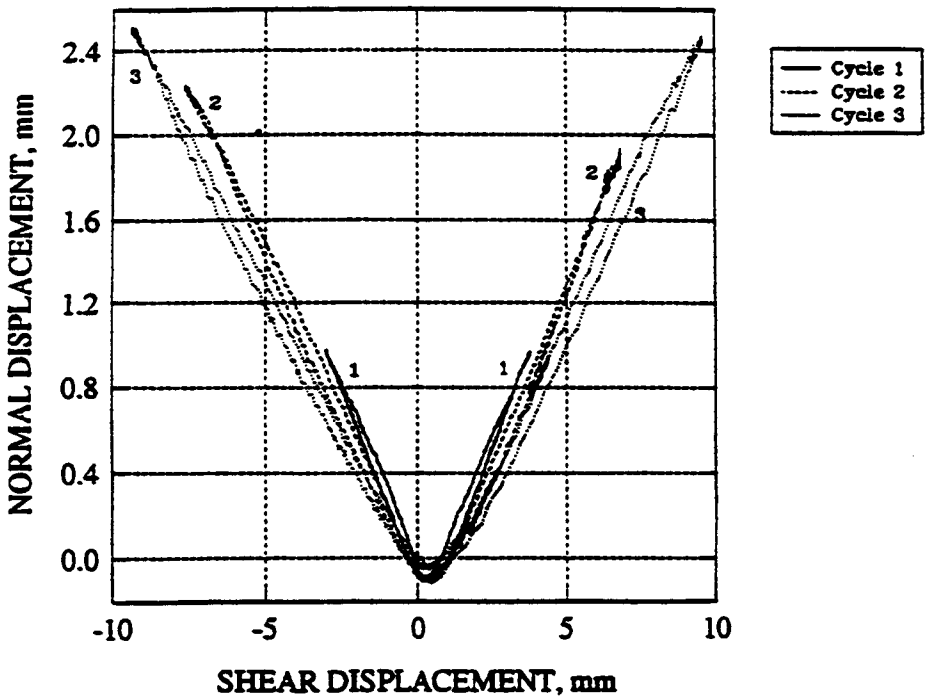


**Figure 2-8. Joint normal displacement (dilation) versus shear displacement of a joint under an earthquake load with a maximum input displacement amplitude of 25.4 mm**

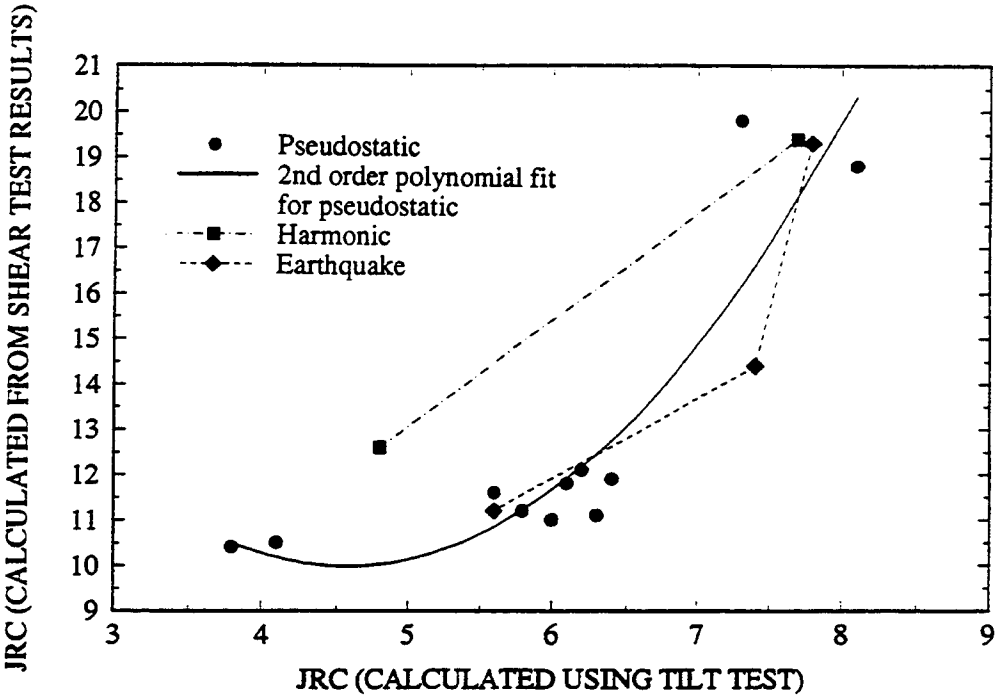


**Figure 2-9. Effect of input frequency (shearing velocity) on peak joint shear strength**

grossly underestimates the real JRC value (Hsiung et al., 1994a), it has been shown through the Spearman's rank correlation coefficient test that the JRC value from the tilt test has a strong positive correlation with the corresponding JRC values calculated from the pseudostatic cyclic shear test results with a correlation coefficient, $R^2$, of about 0.85 (Hsiung et al., 1994a). Therefore, it is possible to develop an empirical expression relating the JRC values from the two methods. The solid line in Figure 2-9 shows a second-order polynomial fit between JRC values from the pseudostatic cyclic test results and the corresponding JRC from tilt tests with an $R^2$ of 0.82. This polynomial fit should provide sufficient confidence in estimating the JRC for the Apache Leap tuff joints using the tilt test. Subsequently, the estimated JRC can be used to estimate the "pseudostatic" peak joint shear resistance with reasonable confidence. Assuming that the peak joint shear strength will be affected by dynamic loads (e.g., induce a higher peak shear strength than the peak shear strength if the same specimen was tested under pseudostatic condition), then the JRC value calculated from the "dynamic" joint shear strength should be larger than the JRC value from the pseudostatic shear strength. In other words, the dynamic JRC should fall above the second-order polynomial curve if plotted in Figure 2-9. Figure 2-9 includes the dynamic JRC from the harmonic and earthquake test results. Examination of the figure indicates that, in general, the dynamic JRC values do not differ significantly from the corresponding pseudostatic JRC values, except for one data point from a harmonic test result. This observation is an indication that the shear velocity input may not have an appreciable influence on the peak joint shear strength.

Figure 2-10 shows the effect of joint roughness on joint shear stress reduction during reverse shearing for the dynamic test. The horizontal axis represents the JRC values that were calculated using the dynamic peak shear strength results. The vertical axis is the ratio of the approximate shear strength during reverse shearing to the corresponding peak shear strength for forward shearing. There are two curves for each type of dynamic test in the figure. The legend Earthquake, 1 denotes that the data in the

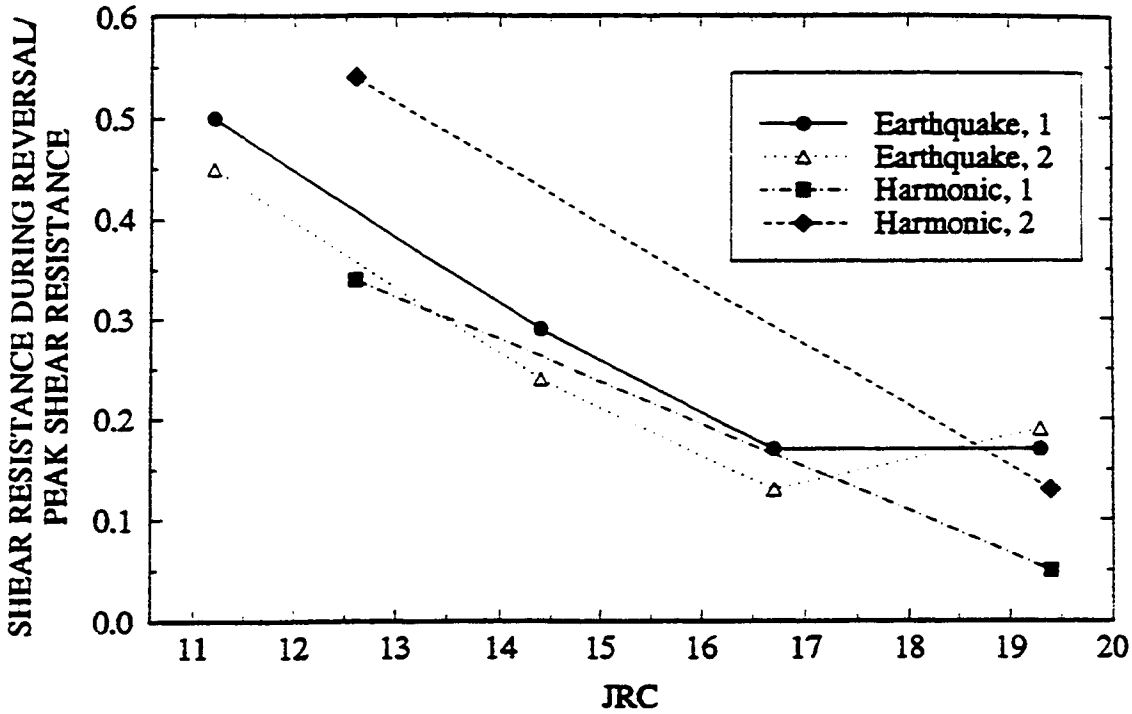


**Figure 2-10. Effect of input frequency (shearing velocity) on joint shear strength during reverse shearing**

1st and 4th quadrants of the shear stress versus shear displacement characteristic curves for the earthquake tests were used, while the legend Earthquake, 2 denotes that the data in the 3rd and 2nd quadrants were used. The same approach was used for the harmonic tests. Figure 2-10 shows that the difference between the joint shear strength during reverse shearing and the peak shear strength will be larger for joints with rougher surfaces. On the other hand, the figure indicates that the effect of shearing velocity on shear resistance is not noticeable in the experimental results.

In summary, within the range of variation, the test input velocity or frequency is found to affect the stick-slip behavior of the Apache Leap tuff joints. As discussed earlier, the stick-slip behavior is believed to have limited effect on joint performance. No noticeable effect of the input frequency on the peak joint shear strength and the joint shear strength for the reverse shearing is observed. Consequently, it is possible to disregard the effect of shearing velocity variations, within a range from a velocity that is equivalent to a static condition to a velocity variation comparable to earthquakes, in evaluating joint behavior. However, the observed differences in joint behavior between reverse shearing and forward shearing, in the sense of joint shear strength, and the joint dilation recovery during reverse shearing deserve adequate representation by the rock joint models.

Commonly used empirical representations of jointed rock behavior reside in the Mohr-Coulomb, Barton-Bandis, and Continuously-Yielding models. These models were developed primarily on the data taken under unidirectional pseudostatic loading conditions, that is only for forward shearing. Careful examination of these three models (Hsiung et al., 1994b) has revealed that all three models have adopted essentially the same principle in determining the joint shear and dilation behavior during reverse shearing. This principle asserts that same joint behavior occurs under both forward and reverse shearing conditions. With this principle, the same shear strength criterion is applicable to both conditions and the joint dilation

continues to increase even during reverse shearing. Consequently, all three models are found not able to adequately predict the joint shear and dilation behavior under reverse shearing (Hsiung et al., 1994b). This inability is clearly due to the lack of understanding of joint cyclic shear behavior and due to a roughness representation used in the models that does not reflect the portion of the joint characteristics controlling the reverse shearing behavior of a rock joint. A new or modified representation for rock joint roughness is apparently needed.

# 3 DEVELOPMENT OF CHARACTERIZATION TECHNIQUE FOR ROCK JOINT ROUGHNESS

It is recognized that an acceptable rock joint model for adequately describing rock joint behavior both under cyclic pseudostatic and dynamic shear conditions will require a suitable measure of rock joint roughness. A commonly used measure of joint roughness in rock engineering practice is the JRC proposed by Barton (1973) and adopted by the ISRM (1978). This JRC concept has been implemented in a rock joint model developed by Barton and Choubey (1977). This rock joint model is able to adequately describe the unidirectional shear and dilation behavior of fresh rock joints (Hsiung et al., 1994b), provided representative JRC values are used. However, as discussed in Chapter 2, this JRC concept does not seem to include the joint characteristics that govern the joint behavior during reverse shearing. Consequently, the rock joint model that utilized this concept cannot be used for the prediction of the reverse shearing behavior of a rock joint. Further, the determination of the JRC value of a rock joint profile is highly subjective (Miller et al., 1989) since as originally proposed by Barton and Choubey (1977), it is done by visually matching the joint surface profile with the ten "standard" profiles whose JRC values range from 0 to 20. Several methods have been proposed to link the JRC value with various aspects of the statistical characteristics of a rock joint to provide an objective alternate for JRC determination. These methods were evaluated by Hsiung et al. (1993) and were found to underestimate the JRC value of a rock joint by a substantial amount. Furthermore, none of these methods have included all aspects of joint characteristics.

One of the approaches for analyzing rock joint profiles is the theory of fractal geometry. Several researchers proposed equations that correlate JRC values (which range from 0 to 20) of the ten standard profiles to their fractal dimensions. (It will be shown later in this chapter that fractal dimension alone is not sufficient to uniquely define a joint profile) In the process of determining their fractal dimensions, the ten standard profiles were assumed to be self-similar (Turk et al., 1987; Lee et al., 1990; Wakabayashi and Fukushige, 1992). The assumption that rock joint profiles are self-similar implies that each profile is composed of several copies of itself with possible rotation and translation, scaled down from the original by a constant ratio $r$ in all spatial directions. However, in reality, studies have shown that rock profiles or surface topographies are often self-affine fractals (Brown and Scholz, 1985; Brown, 1987; Malinverno, 1990) and will require different scaling factors in different directions. Formally, points $X = (x,y)$ transform into new points $X' = (r_x x, r_y y)$ with $r_x = r_y^H$ where H is the Hurst exponent and ranges between 0 and 1. Furthermore, these existing equations developed based on self-similar fractal geometry have been shown to have considerably underestimated the JRC values for natural rock joint profiles (Hsiung et al. 1993).

In the study reported herein, the theory of self-affine fractal geometry is adopted to characterize the ten standard profiles, since this theory provides a sound mathematical basis and can capture uniquely the characteristics of a fractal object (rock profile). The profiles are treated to be self-affine instead of self-similar. The objective of this characterization is to obtain a better understanding of the ten profiles and to establish a relationship between the fractal properties of the profiles with their associated JRC values, if such a relation exists. Since a relationship exists between JRC and rock joint model parameters such as friction angle and joint degradation, this approach will lead to the establishment of a relationship between fractal properties and rock joint parameters. Several methods are available for calculating the properties of a self-affine fractal. Four such methods were used in this study. These are the divider method, variogram method, spectral method, and RMS method.

## 3.1 DIVIDER METHOD

Given an object is divided into N smaller objects each with a size or divider length R, the divider method calculates the fractal dimension D with (Mandelbrot, 1982; Feder, 1988):

$$N = R^{-D} \tag{3-1}$$

However, the dimension of a self-affine fractal may not be uniquely defined using the above equation (Mandelbrot, 1982), if the divider length is too large compared to the roughness of the fractal object. In this regard, the fractal dimension obtained should approach the topological dimension, that is $D \simeq 1.0$. This means, in a global sense, that the object is not fractal. But in a local sense, that is, using a small divider length compared to the fluctuation, the divider dimension can be defined as (Feder, 1988):

$$D_D = \frac{1}{H} \tag{3-2}$$

This behavior of the self-affine fractal involves a crossover value of the sample interval where the local value of the fractal dimension passes to a global one. The existence of a crossover value makes the determination of fractal dimension of a self-affine fractal object difficult since the sampling interval for a data set is normally much greater than this crossover value. To overcome this difficulty, Brown (1987) has suggested an alternative by magnifying the profile height repeatedly by various factors then using the divider method until a stable fractal dimension is obtained. Applying this alternative, this study indicates that the calculated fractal dimension increases as the magnification factor increases until a maximum fractal dimension value is reached. Further increasing the magnification factor results in a decrease in fractal dimension. The idea of magnifying a profile height (equivalent to reducing divider lengths) is to create a distinct contrast between the total lengths calculated using various divider lengths (that is, to increase the difference between the total lengths) so that a reasonable fractal dimension can be obtained. This approach will only work when the "equivalent" divider lengths are within a range that is comparable to the crossover length (perhaps, within one or two orders of magnitude). Such contrast will begin to diminish as the magnification factor continues to increase since the total lengths calculated for various divider lengths will eventually be equal.

## 3.2 VARIOGRAM METHOD

Variogram or semi-variogram is used to characterize the spatial variability of random functions and it is extremely well-suited for describing random functions that are second-order stationary or appear to vary without bound (Journel and Huijbregts, 1978; Oliver and Webster, 1986). The variogram function is defined as the average of the sum of the squares of the profile height differences separated by a given lag. The one-dimensional variogram function, $\gamma(h)$, can be expressed in a discrete form:

$$\gamma(h) = \frac{1}{2N} \sum_{i=1}^{N} \left[Z(x_i) - Z(x_i + h)\right]^2 \tag{3-3}$$

where $Z(x_i)$ is the height of the profile at location $x_i$, $Z(x_i+h)$ is the height of the profile at location $x_i+h$, h is the lag between two points, and N is the number of observations. A plot of the variogram function versus the lag, h, will reveal a suite of information regarding the characteristics of the profile.

However, they are not the focus of discussion in this report. The fractal dimension of a profile can be determined from the initial slope, $\beta$, of the log-log plot of the variogram function versus the lag, using the equation, $D = 2 - \beta/2$.

## 3.3 SPECTRAL METHOD

The spectral method has been widely used for fractal dimension determination of a self-affine fractal object (Brown and Scholz, 1985; Power and Tullis, 1991). When an object or a profile is fractal, the slope of the power spectral density (PSD) of the profile will not vary with the cutoff frequency. PSD curves of fractals can be approximated by

$$S(f) = af^{-\beta} \tag{3-4}$$

where S(f) is the PSD, a is a constant, and f is the frequency. The fractal dimension can be calculated from $D = (5 - \beta)/2$. All data used in this study were detrended before they were analyzed with the spectral method.

## 3.4 ROUGHNESS-LENGTH (RMS) METHOD

The RMS method was proposed by Malinverno (1990). This method measures the profile roughness as the root-mean-square value of the residuals on a linear trend fitted to the sample data points in a window of length $w$. The removal of this local trend is necessary to avoid overestimating roughness in small windows since small samples contain significant trends, due to the presence of the powerful long wavelength, although self-affine series tend to be flat on large scales (Malinverno, 1990). The RMS roughness can be calculated by

$$\mathrm{RMS}(w) = \frac{1}{n_w} \sum_{i=1}^{n_w} \sqrt{\frac{1}{m_i - 2} \sum_{j \in w_i} (z_j - z)} \tag{3-5}$$

where $n_w$ is the total number of windows of length w, $m_i$ is the number of points in window $w_i$, $z_j$ is the residual on the trend, and z is the mean residual in window $w_i$. The fractal dimension from this method can be obtained from $D = 2 - \beta$, where $\beta$ is the slope of the log-log plot of the RMS(w) function versus the window length w.

## 3.5 METHOD VERIFICATION

FORTRAN computer programs based on these four methods were written for fractal dimension calculation. Fractional Brownian motion functions with known fractal dimensions were used to verify the validity of these programs. Generation of the fractional Brownian motion functions used the algorithm proposed by Saupe (1988). Five Hurst exponent H values ranging from 0.5 to 0.9 were chosen to generate the fractional Brownian motion functions that have fractal dimensions D from 1.1 to 1.5, where $D = 2 - H$.

Figure 3-1 shows the comparison of the H values calculated from the four programs with the actual H values used to generate the Brownian motion functions. There is difference among the predictions of fractal dimensions from the various methods. However, it can be concluded from the figure

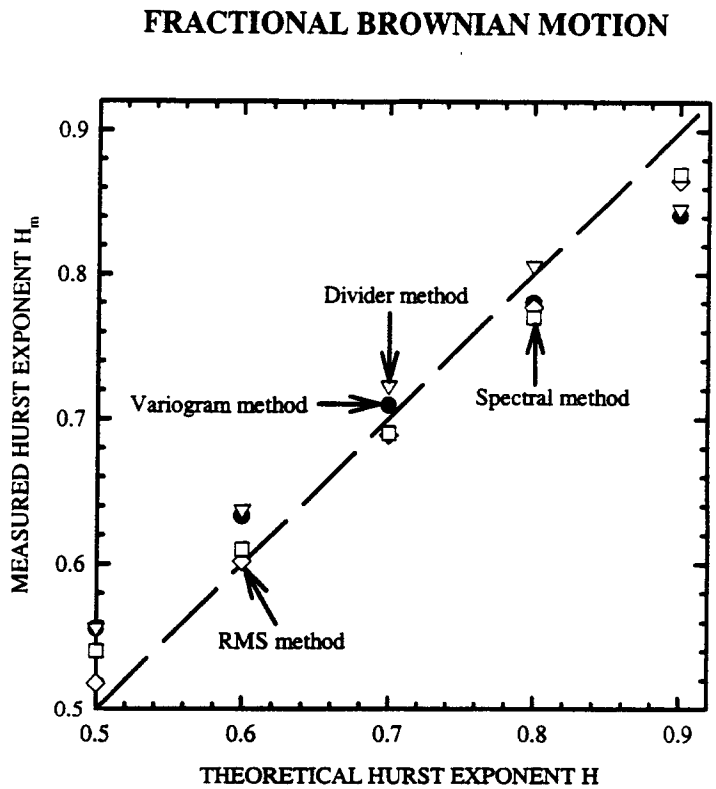


**Figure 3-1. Comparison of Hurst exponents calculated using the four methods with the expected values**

that all four methods estimate reasonably well the H value of each Brownian motion function, although there is a slight overestimation for rougher Brownian motion functions (corresponding to smaller H values), and underestimation for smoother Brownian motion functions (corresponding to larger H values) recognizing that self-affinity is intrinsically difficult to measure on a finite sample. The fact that all four methods yield fairly good predictions gives the authors reasonable confidence in applying these methods to analyzing Barton's ten standard profiles.

## 3.6 EVALUATION OF BARTON'S TEN PROFILES

As discussed earlier, the JRC value is the most commonly used measure for representing joint roughness. The proposed ten profiles (Barton, 1973; ISRM, 1978) represent JRC values from 0 to 20. Each profile covers a range of two scales of JRC; for example, from 0 to 2. In this study, a unique value (middle value of a range) was assigned to each profile for practicality.

The plot of the ten profiles contained in the ISRM (1978) publication was magnified using a photocopier to about 3 times the size of the original plot for ease of digitization. The enlarged profiles were then digitized individually to create ten data sets. The upper boundary of each curve was used as a basis for digitizing. Only local peaks and valleys were digitized to give coordinates with respect to a selected horizontal datum. Consequently, the data interval in each of the data sets was not constant. For most of the profile curves, more than 300 points (locations) were digitized. The same unit length was

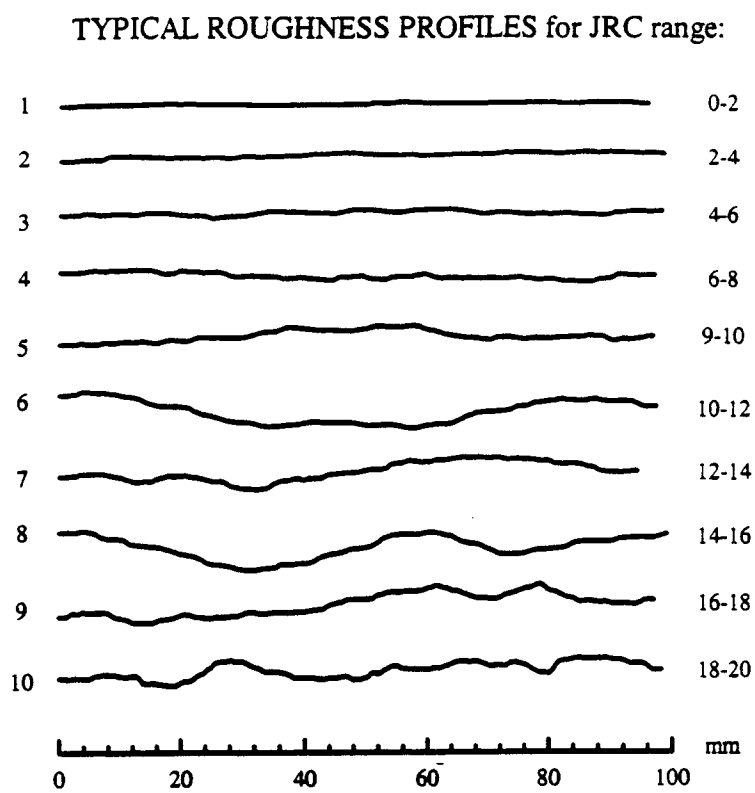


**Figure 3-2. Roughness profiles and the corresponding range of *JRC* values**

used for both the horizontal and vertical axes. A FORTRAN program was developed to re-scale the data using the interpolating technique such that each data set has an equal data spacing and contains 512 data points. Equal spacing is necessary for using the spectral and variogram methods and the 512 value is the 7th power of 2, which greatly simplifies the Fourier transform procedure used in the spectral method. Figure 3-2 shows the plot of the ten standard profiles regenerated using the final data sets. Comparison of the ten profile curves with the corresponding ones in the original ISRM (1978) publication shows a remarkable similarity and can be considered representative.

Figure 3-3 shows the relation of the JRC values of the ten profiles and the corresponding fractal dimensions from the four methods. Contrary to common belief that a larger fractal dimension should correspond to a higher JRC value, Figure 3-3 shows that all four methods consistently predict a decreasing trend of the JRC values with increase in fractal dimension. Similar results were also reported by Sakellariou et al. (1991). They also used the spectral method to calculate the fractal dimensions of the ten profiles. Although the fractal dimensions reported by them do not show a distinct decreasing trend, they did report unusually high fractal dimensions for the first five profiles. Sakellariou et al. (1991) considered these relatively high values as erratic behavior and suggested that this behavior may be explained by the "quality of source material (smooth figures of a book) that causes mixing of noise in the signal in the raw data, a fact that cannot be overcome." While their postulation, in general, may be correct, it cannot explain the distinct and consistent trend of decreasing fractal dimension with increasing JRC value observed in Figure 3-3. Figure 3-3 also indicates that the fractal dimensions calculated from different methods are quite different, with the results from the spectral method differing the most. This is consistent with the result shown in Figure 3-1. The differences among the fractal dimensions calculated

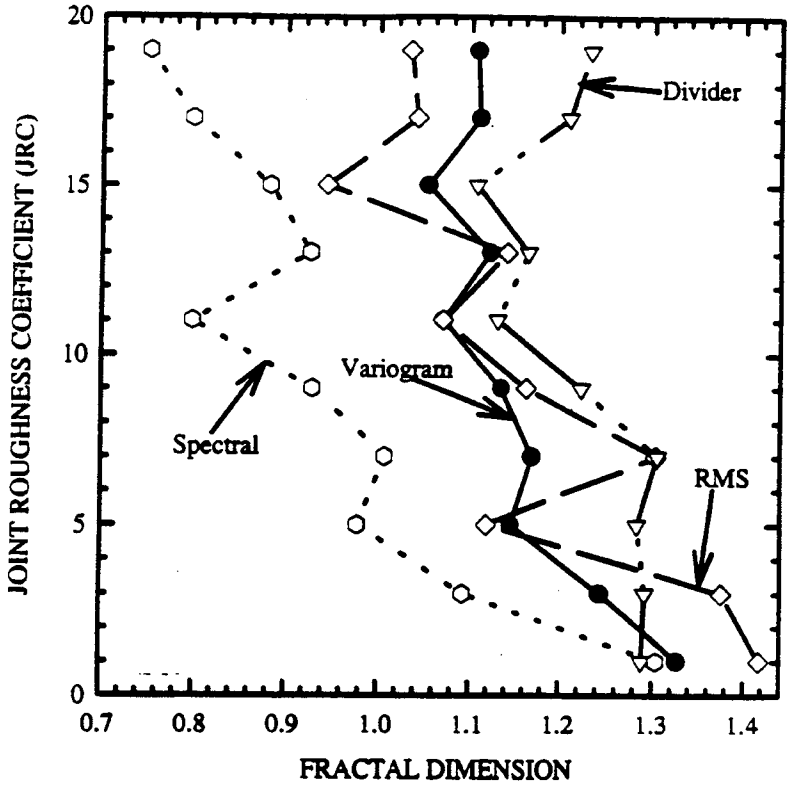


**Figure 3-3. Relation of *JRC* and the corresponding fractal dimension calculated from four different methods**

from the variogram and divider methods for the ten profiles are relatively small compared to those from the RMS and spectral methods. Except for the first two and the fourth profiles (Figure 3-2), the fractal dimensions calculated using the spectral method were smaller than one, which is physically unrealistic. The reason for this phenomenon is currently not clear.

The finding that a higher JRC value corresponds to a smaller fractal dimension suggests that the use of fractal dimension alone for the characterization of the ten profiles is not sufficient since, according to the conventional wisdom, a rougher surface should yield a larger fractal dimension. Also the fractal dimension only describes how the roughness varies with the scale of observation. It is the intercept, for example, the constant a in Eq. (3-4), or the crossover length that determines the steepness (or the total variability) of the topography (Power and Tullis, 1991). Consequently, both the fractal dimension and the intercept are needed to uniquely define a profile curve.

Figures 3-4, 3-5, and 3-6 show the log-log plots of the fractal models for the ten profiles using the variogram, spectral, and RMS methods, respectively. The log-log plot of the fractal models using the divider method is not constructed since a different magnification factor was used for each of the ten profiles, which makes a meaningful direct comparison impossible. The crossover length of each profile was not calculated in this study since it lies outside the range in which the data were collected. The fact that the crossover length is outside the range could make the interpretation of the crossover length difficult and potentially problematic (Power and Tullis, 1991). However, even without this information, the plots of fractal models yield significant insight regarding evaluation of the ten profiles.

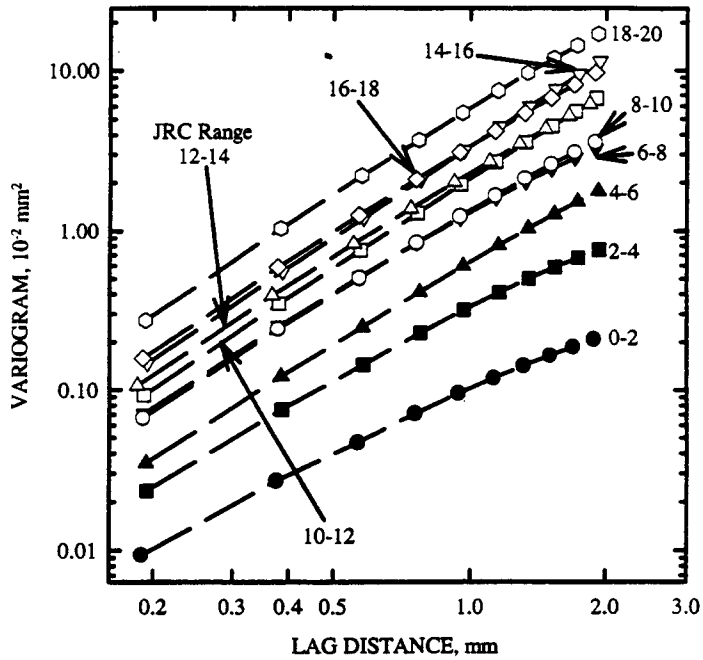


**Figure 3-4. Plot of fractal models for Barton's ten profiles from the variogram method**

As can be observed in Figures 3-4, 3-5, and 3-6, a profile with a higher JRC value, in general, tends to have a larger intercept; an indication that this profile is steeper in topography and consequently is rougher. This observation seems to suggest that the intercept of a fractal model may be an appropriate parameter in addition to the fractal dimension in characterizing the roughness of a profile surface. In essence, the intercept, to a certain extent, may be related to the local trend (long wavelengths) associated with a profile. This local trend was found to be the controlling parameter in shearing behavior of rock joints at laboratory scales by Jing et al. (1992) and Hsiung et al. (1994a). They defined this local trend as primary asperities. The fractal dimension, on the other hand, may be related to the higher order asperities of the profile that have only a secondary effect on the shearing behavior of rock joints. A further study in this area to relate the intercept and fractal dimension of a rock profile to friction properties of the profile that can be used to predict the shearing behavior of the rock joint is in progress.

The fractal models generated using the variogram method (Figure 3-4) seem to provide more insight regarding the fractal characters of the ten profiles than those from the spectral and RMS methods (Figures 3-5 and 3-6). Although the ten profiles are, in general, in the right order in terms of roughness according to Figure 3-4, not all the proposed profiles are representative of the suggested roughness classes. For example, the fractal models for the profiles with JRC values in the ranges of 6–8 and 8–10 are almost identical. The same is true of the two profiles with JRC of 14–16 and 16–18. Although there is a slight difference between the two profiles with JRC of 10–12 and 12–14, for practical purposes they may be judged to be the same. Consequently, the fractal analysis using the variogram method seems to suggest that the ten profiles may be reduced to seven; that is, for JRC range from 0–2, 2–4, 4–6, 6–10, 10–14, 14–18, and 18–20. The fractal analyses using the spectral and RMS methods do not show such a clear trend. However, these analyses do suggest that the distinctions among the roughnesses for at least five profiles with JRC ranging from 6–16 are not clear cut.

BARTON'S STANDARD PROFILE, SPECTRAL APPROACH

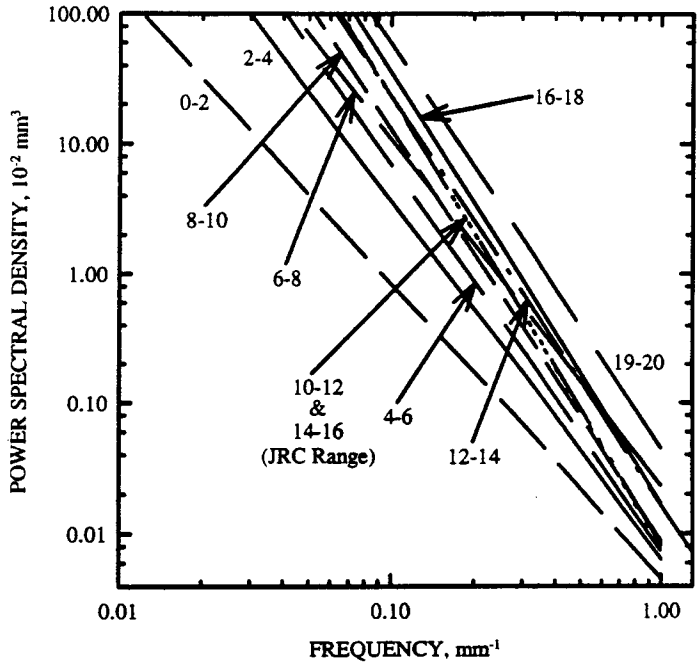


**Figure 3-5. Plot of fractal models for Barton's ten profiles from the spectral method**

BARTON'S STANDARD PROFILES, RMS APPROACH

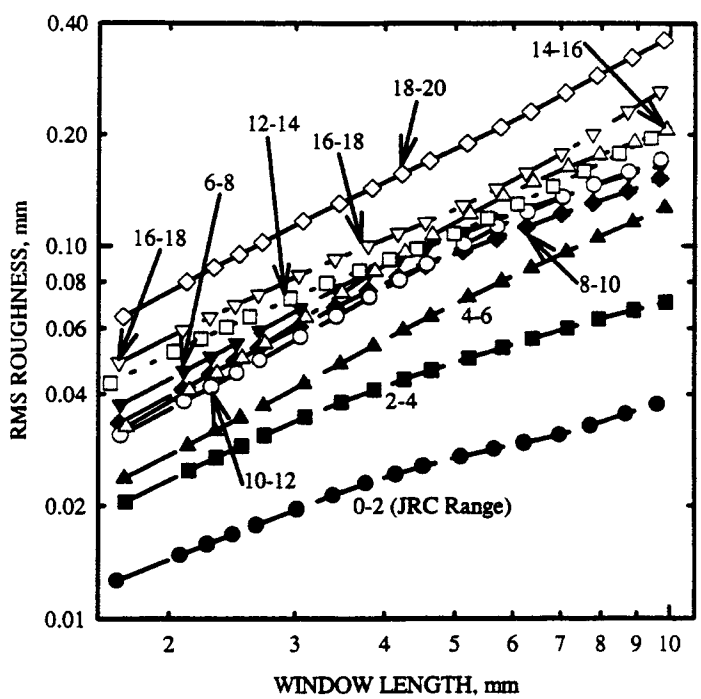


**Figure 3-6. Plot of fractal models for Barton's ten profiles from the RMS method**

# 4 NEED FOR ALTERNATIVE APPROACH

As a part of the overall approach to developing a rock joint model to predict joint behavior under cyclic loading conditions, a technique for joint roughness characterization that relates the fractal properties (fractal dimension and intercept) to the commonly used JRC concept is being studied. This approach offers some distinct advantages. As discussed earlier, the JRC concept is well accepted as a means for representating the surface roughness and the rock joint model developed by Barton and Choubey (1977) that utilizes this concept has demonstrated, on many occasions, its ability to adequately describe the unidirectional shear behavior of fresh rock joints (Barton and Bandis, 1982; Barton et al., 1985; Hsiung, et al., 1994b), provided representative JRC values are used. By establishing a relation between the joint fractal properties and the corresponding JRC value, this rock joint model can be used as a basis for our model development work, recognizing that a correct mechanism for joint reverse shearing behavior will have to be included. This approach will minimize the amount of effort necessary for the model development work.

As discussed in Chapter 3, the study of the self-affine fractal properties of Barton's ten standard profiles has found that not all these profiles are representative of the suggested roughness classes. At least five profiles with the suggested JRC values ranging from 6–16 do not show distinct differences in their fractal properties (Figures 3-4, 3-5, and 3-6). This is not too surprising because the original intent of the ten profiles was to provide a quick estimation of joint roughness in the field. This estimation is done by approximating the JRC values of joint surfaces through visually matching these surface profiles with the ten standard ones so that a timely judgment can be made for solving pressing rock engineering problems. Therefore, it is understandable if these standard profiles are not rigorous. However, this observation does prevent establishing a valid systematic relationship between the fractal properties and JRC values of the ten profiles. This matter is further complicated by the fact that the four methods used for characterizing the fractal properties generate somewhat inconsistent results because each method tends to focus on a slightly different aspect of a fractal object. This difference can be substantiated by comparing the fractal models plotted in Figures 3-4, 3-5, and 3-6 for the profiles with JRC values ranging from 6–16. The fundamental differences among these methods for fractal characterization are not well-understood.

Given the discussions provided earlier, it is considered that an alternate approach is necessary for relating the roughness of a joint surface with the associated fractal properties (fractal dimension and intercept). The authors are currently studying the feasibility of two possible approaches. The first approach, which is preferred, is to still use the JRC concept but to modify the standard profiles with JRC values between 6–16 as appropriate. The second approach calls for reformulating the JRC concept. This would involve developing a new basis for correlating joint characteristics, in terms of fractal dimensions and intercepts, of approximately 30 Apache Leap tuff rock joint specimens tested at cyclic pseudostatic and dynamic shear conditions at the CNWRA with the corresponding experimental results on joint shear strength (Hsiung et al., 1994a). It appears that first approach will require less effort than the second. Furthermore, the cyclic pseudostatic and dynamic experimental results can be reserved for use for verifying the rock joint model if the first approach is used. The applicability of the rock joint model that may be developed by following the first approach will be limited to JRC values of 20 or less as in the case of the Barton-Bandis rock joint model (Barton et al., 1985). The average JRC value of each Apache Leap tuff joint surface tested to date has been less than 20 (Hsiung et al., 1993), although the JRC value along an individual line of the joint surface may be larger than 20. The joint model developed using the second approach on the other hand will limit its application to a somewhat narrower JRC range, approximately 7-20 (Hsiung et al., 1993), as compared to that based on the first approach. Expanding usage of this model outside the JRC range (7-20) will involve some uncertainty. Furthermore verification of this model can be problematic since most or all experimental results need to be used for model development.

# 5 SUMMARY

The ten standard profiles associated with the JRC concept were analyzed using the theory of fractal geometry. The divider, variogram, spectral, and RMS methods were evaluated. The results from all four methods show a consistent trend that a profile with a higher JRC value seems to have a smaller fractal dimension. Consequently, using fractal dimension alone may not be sufficient for characterizing the roughness of a rock joint for engineering purposes. The intercept of the fractal model of a profile is found to be representative of the primary asperities with long wavelengths (local trend) that are believed to control the actual shear behavior of rock joints at laboratory scales. To uniquely define a joint profile, both the fractal dimension and the intercept are needed. Even considering these two parameters, this study has shown that not all of the profiles are representative of the roughness classes that were proposed by Barton (1973). Therefore, it is not possible to establish a valid systematic relationship between the fractal properties and the JRC value of the ten profiles.

An alternate approach is necessary for relating the roughness of a joint surface and its fractal properties. Two alternate approaches are currently under study. One is to modify the standard profile with JRC values between 6–16, as appropriate. The other is to develop a new basis for correlating the fractal dimension and intercept of a joint with its friction angle. The first approach offers certain advantages over the second. However, the applicability of the rock joint model that may be developed by following the first approach will be limited to JRC values of 20 or less, as in the case of the Barton-Bandis rock joint model (Barton et al., 1985)

# 6 REFERENCES


Barton, N.R. 1973. Review of a New Shear Strength Criterion for Rock Joints. *Engineering Geology* 7:287–332.

Barton, N.R., and S.C. Bandis. 1982. Effects of block size on the shear behavior of jointed rock. *23rd U.S. Symposium on Rock Mechanics*. University of California at Berkeley. Berkeley, CA.

Barton, N.R., S.C. Bandis, and K. Bakhtar. 1985. Strength, deformation and conductivity coupling of rock joints. *International Journal of Rock Mechanics and Mining Sciences & Geomechanics Abstracts* 22(3):121–140.

Barton N.R., and V. Choubey. 1977. The shear strength of rock joints in theory and practice. *Rock Mechanics* 10:1–54.

Brown, S.R., and C.H. Scholz. 1985. Broad bandwidth study of the topography of natural rock surfaces. *Journal of Geophysical Research* 90(B14):12,575–12,582.

Brown, S.R. 1987. A note on the description of surface roughness using fractal dimension. *Geophysical Research Let.* 14(11):1,095–1,098.

Feder, J. 1988. *Fractals*. Plenum Press, New York.

Hsiung, S.M., W. Blake, A.H. Chowdhury, and T.J. Williams. 1992a. Effects of mining-induced seismic events on a deep underground mine. *Pure and Applied Geophysics* 139:741–762.

Hsiung, S.M., A.H. Chowdhury, W. Blake, M.P. Ahola, and A. Ghosh. 1992b. *Field Site Investigation: Effect of Mine Seismicity on a Jointed Rock Mass*. CNWRA 92-012. San Antonio, TX: Center for Nuclear Waste Regulatory Analyses.

Hsiung, S.M., A. Ghosh, M.P. Ahola, and A.H. Chowdhury. 1993. Assessment of conventional methodologies for joint roughness coefficient determination. *International Journal of rock Mechanics and Mining Sciences & Geomechanics Abstracts* 30(7): 825–829.

Hsiung, S.M., M.P. Ahola, A.H. Chowdhury, and A. Ghosh. 1994a. *Laboratory Characterization on Rock Joints*. NUREG/CR-6178. Washington, DC: Nuclear Regulatory Commission.

Hsiung, S.M., A. Ghosh, A.H. Chowdhury, and M.P. Ahola. 1994b. *Evaluation of Rock Joint Models and Computer Code UDEC Against Experimental Results*. NUREG/CR-6216. Washington, DC: Nuclear Regulatory Commission.

Huang, X., B.C. Haimson, M.E. Plesha, and X. Qiu. 1993. An investigation of the mechanics of rock joints—part I. Laboratory investigation. *International Journal of Rock Mechanics and Mining Sciences & Geomechanics Abstracts* 30(3): 257–269.

International Society for Rock Mechanics (ISRM). 1978. Suggested methods for the quantitative description of discontinuities in rock masses. *International Journal of Rock Mechanics and Mining Sciences & Geomechanics Abstracts* 15:319–368.

Jing, L., E. Nordlund, and O. Stephansson. 1992. An experimental study on the anisotropy and stress-dependency of the strength and deformability of rock joints. *International Journal of Rock Mechanics and Mining Sciences & Geomechanics Abstracts* 29(6):535–542.

Journel, A., and J. Huijbregts. 1978. *Mining Geostatistics*. Academic Press, New York.

Kana, D.D., B.H.G. Brady, B.W. Vanzant, and P.K. Nair. 1991. *Critical Assessment of Seismic and Geomechanics Literature Related to a High-Level Nuclear Waste Underground Repository*. NUREG/CR-5440. Washington, DC: Nuclear Regulatory Commission.

Lee, Y.-H., J.R. Carr, D.J. Barr, and C.J. Haas. 1990. The fractal dimension as a measure of the roughness of rock discontinuity profiles. *International Journal of Rock Mechanics and Mining Sciences & Geomechanics Abstracts* 27:453–464.

Malinverno, A. 1990. A simple method to estimate the fractal dimension of a self-affine series. *Geophys. Res. Let.* 17(11):1,953–1,956.

Mandelbrot, B.B. 1982. *The Fractal Geometry of Nature*. Freeman, San Francisco, CA.

Miller, S.M., P.C. McWilliam, and J.C. Kerkering. 1989. Evaluation of stereo digitizing rock fracture roughness. *Rock Mechanics as a Guide for Efficient Utilization of Natural Resources*. A.W. Khair, ed., Balkema, Rotterdam 201–208.

Nuclear Waste Technical Review Board. 1992. *Fifth Report to the U.S. Congress and the U.S. Secretary of Energy*. Washington, DC: U.S. Government Printing Office.

Oliver, M.A., and R. Webster. 1986. Semi-variograms for modelling the spatial pattern of landform and soil properties. *Earth Surface Processes and Landforms* 11:491–504.

Power, W.L., and T.E. Tullis. 1991. Euclidean and fractal models for the description of rock surface roughness. *J. Geophys. Res* 96(B1):415–424.

Sakellariou, M., B. Nakos, and C. Mitsakaki. 1991. On the fractal character of rough surfaces. *International Journal of Rock Mechanics and Mining Sciences & Geomechanics Abstracts* 28(6): 527–533.

Saupe, D. 1988. Algorithms for random fractals. *The Science of Fractal Images*. H. Peitgen and D. Saupe, eds., Springer-Verlag, New York: 71–136.

Turk N., J.M. Greig, W.R. Dearman, and F.F. Amin. 1987. Characterization of rock joint surfaces by fractal dimension. *28th U.S. Symposium on Rock Mechanics*. University of Arizona 1,223–1,236.

Wakabayashi, N. and I. Fukushige. 1992. Experimental study on the relation between fractal dimension and shear strength. *Conference of Fractured and Jointed Rock Masses*. Preprints. Lawrence Berkeley National Laboratory: Lake Tahoe, CA.

Wibowo, J.T., B. Amadei, S. Sture, and A.B. Robertson. 1992. Shear response of a rock joint under different boundary conditions: An experimental study. *Conference of Fractured and Jointed Rock Masses*. Preprints. Lawrence Berkeley National Laboratory: Lake Tahoe, CA.